

Comparative study between neural hysteresis, fuzzy PI, and neural switching table for an IM DTC control

Habib Benbouhenni, Zinelaabidine Boudjema

Abstract— Direct torque control (DTC) has gained popularity for development of advanced AC machines control due to its simplicity and offers fast instantaneous torque and flux controls. This paper proposes five DTC schemes that will be compared with each other. These five schemes are classical DTC, DTC with fuzzy PI controller, DTC with neural hysteresis, DTC with artificial neural network (DTC-ANN) and neural hysteresis DTC with fuzzy PI speed controller. In other hand, this paper presents an improved switching strategy for reducing flux and torque ripples in DTC of induction machine (IM) drives. It can be shown that the new switching table DTC-ANN while the reduction of torque ripples, stator flux ripples and THD value of stator current. The validity of the proposed methods is confirmed by the simulation results.

Keywords— DTC, IM, Fuzzy PI controller, Artificial neural network, Neural hysteresis comparators, THD.

I. INTRODUCTION

To day, high dynamic performances of IM drives is indispensable in many industrial applications. IM control has attracted much attention recently in the power electronics field. Vector control based on rotor flux orientation presents a major disadvantage to be relatively sensible to the machine parameters variation [1].

For such reasons, DTC method was proposed in the middle of 1980 by I. Takahashi. This method has become one of the high performance control strategies for AC machine to provide a very fast torque and flux control. The name direct torque control is derived by the fact that, on the basis of the errors between the reference and the estimated values of torque and flux, it is possible to directly control the inverter states in order to reduce the torque and flux errors within the prefixed band limits [2].

Habib Benbouhenni is with the Laboratoire d'Automatique et d'Analyse des Systèmes (LAAS), Département de Génie Electrique, Ecole Nationale Polytechnique d'Oran, Maurice Audin, Oran, Algeria. habib0264@gmail.com

Zinelaabidine Boudjema is with the Laboratoire Génie Electrique et Energies Renouvelables (LGEER), Electrical Engineering Department, Hassiba Benbouali University, Chlef, Algeria. Boudjema1983@yahoo.fr

DTC method is characterised by its simple implementation and fast dynamic responses. Furthermore, the inverter is directly controlled by the algorithm, i.e. a modulation technique for the inverter is not needed. The main advantages of DTC are the absence of coordinate transformation and current regulator, absence of separate voltage modulation block.

Common disadvantages of conventional DTC are high torque ripple, it also needs flux and torque estimators and therefore, accurate machine parameters are required. For that reason the application of artificial neural network attracts the attention of many scientists in the world. The reason for this trend is the many advantages which the architectures of ANN have over traditional algorithmic methods [3].

This paper proposes a new switching table of DTC control to improve the drive performance using neural hysteresis, fuzzy PI controller (Fuzzy neural switching table). The proposed controls schemes is verified by simulation results.

II. THE IM MODEL

By using the definitions of the fluxes, currents and voltages space vectors, the dynamic equations of the three-phase IM in stationary reference frame can be given by the following mathematical form [4]:

$$\overline{V}_s = R_s \overline{I}_s + \frac{d\overline{\Phi}_s}{dt} \quad (1)$$

$$0 = R_r \overline{I}_r + \frac{d\overline{\Phi}_r}{dt} - jWm \overline{\Phi}_r \quad (2)$$

$$\overline{\Phi}_s = L_s \overline{I}_s + M \overline{I}_r \quad (3)$$

$$\overline{\Phi}_r = L_r \overline{I}_r + M \overline{I}_s \quad (4)$$

Where \overline{V}_s is the stator voltage space vector, \overline{i}_s and \overline{i}_r are the stator and rotor currents space vectors, respectively, $\overline{\Phi}_s$ and $\overline{\Phi}_r$ are the stator and rotor flux space vectors, ω is the rotor angular speed, R_s and R_r are the stator and rotor resistances, L_s and L_r are the stator, rotor and mutual inductance, respectively.

The electromagnetic torque is expressed in terms of the cross product of the stator and the rotor flux space vectors.

$$T_e = \frac{3}{2} p \frac{M}{L_r.L_s.\sigma} \vec{\Phi}_r \vec{\Phi}_s \quad (5)$$

$$T_e = \frac{3}{2} p \frac{M}{L_r.L_s.\sigma} \|\vec{\Phi}_s\| \|\vec{\Phi}_r\| \sin(\gamma) \quad (6)$$

Where γ is the load angle between stator and rotor flux space vectors, p is the number of pole pairs of the motor and $\sigma = 1 - \frac{M^2}{L_r.L_s}$ is the dispersion factor.

III. VOLTAGE SOURCE INVERTER MODELING

In The voltage source inverter (VSI) is a static converter constituted by switching cells generally with transistors or IGBT for high powers (Fig. 1). The operating principle can be expressed by imposing on the machine the voltages with variable amplitude and frequency starting from a standard network 791/1368v-60Hz. Voltages at load neutral point can be given by the following expression [2]:

$$\begin{bmatrix} v_A \\ v_B \\ v_C \end{bmatrix} = \frac{E}{6} \begin{bmatrix} 2 & -1 & -1 \\ -1 & 2 & -1 \\ -1 & -1 & 2 \end{bmatrix} \begin{bmatrix} v_{A_o} \\ v_{B_o} \\ v_{C_o} \end{bmatrix} \quad (7)$$

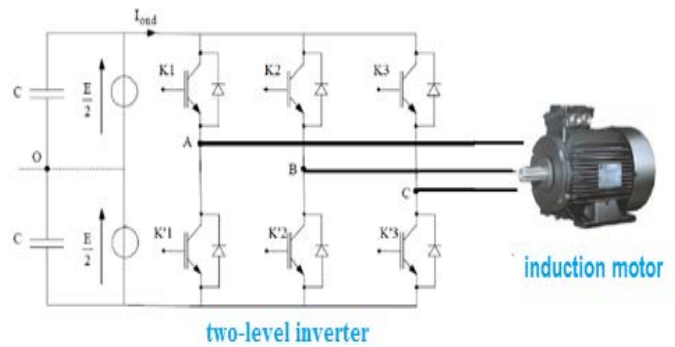


Fig. 1. Voltage source inverter scheme.

IV. TWO-LEVEL DTC

The DTC method allows direct and independent electromagnetic torque and flux control, selecting an optimal switching vector [2]. The Fig. 2 shows the schematic of the basic functional blocks used to implement the DTC of IM drive. A voltage source inverter (VSI) supplies the motor and it is possible to control directly the stator flux and the electromagnetic torque by the selection of optimum inverter switching modes [4].

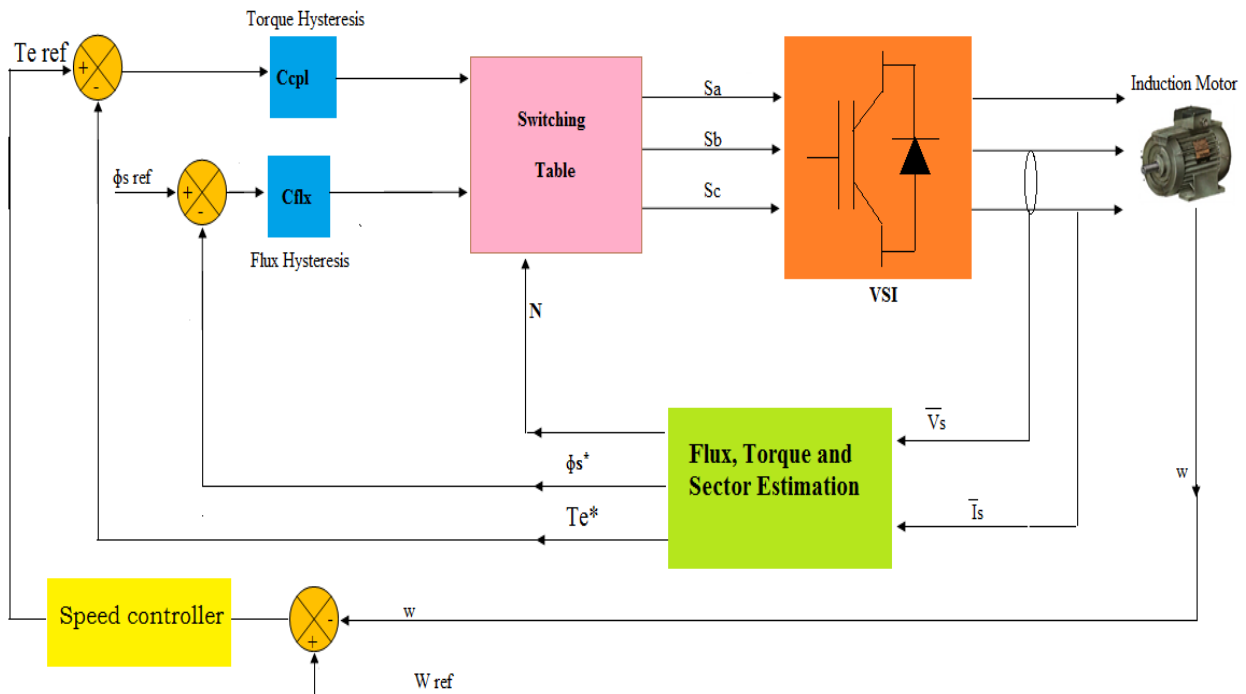


Fig. 2. Basic direct torque control scheme for IM.

This modeling for the two converters that feed the IM.

A. Vector model of inverter output voltage

In the PWM voltage source inverters, considering the combinations of the states of switching functions inverter switching state functions (C1, C2, and C3) which can take either 1 or 0, the voltage vector becomes [5]:

$$v_s = U_0 \cdot \sqrt{\frac{2}{3}} \left(C_1 + C_2 e^{j\frac{2\pi}{3}} + C_3 e^{j\frac{4\pi}{3}} \right) \quad (8)$$

Eight switching combinations can be taken according to the above relationship: two zero voltage vectors and six non-zero voltage vectors show by Fig. 3.

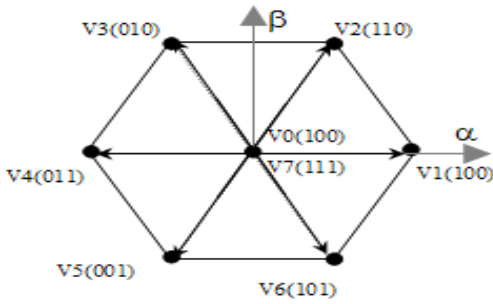


Fig. 3. Partition of the $\alpha\beta$ plane into 6 angular sectors

B. Stator flux and torque estimation

The components of the current ($I_{s\alpha}$, $I_{s\beta}$), and stator voltage ($V_{s\alpha}$, $V_{s\beta}$) are obtained by the application of the transformation given by (9) and (10) [5]:

$$\begin{cases} I_{s\alpha} = I_{sA} \sqrt{\frac{2}{3}} \\ I_{s\beta} = (I_{sB} - I_{sC}) \sqrt{\frac{2}{3}} \end{cases} \quad (9)$$

$$\begin{cases} v_{s\alpha} = U_0 \cdot \left[C_1 - \frac{1}{2}(C_1 + C_2) \right] \sqrt{\frac{2}{3}} \\ v_{s\beta} = \frac{1}{\sqrt{2}} U_0 \cdot (C_2 - C_3) \end{cases} \quad (10)$$

The components of the stator flux ($\Phi_{s\alpha}$, $\Phi_{s\beta}$) are given by (11):

$$\begin{cases} \Phi_{s\alpha} = \int_0^t (v_{s\alpha} - R_s I_s) dt \\ \Phi_{s\beta} = \int_0^t (v_{s\beta} - R_s I_s) dt \end{cases} \quad (11)$$

The stator flux linkage phase is given by (12):

$$\Phi_s = \sqrt{\Phi_{s\beta}^2 + \Phi_{s\alpha}^2} \quad (12)$$

The electromagnetic torque can be obtained starting from the estimated sizes of flux ($\Phi_{s\alpha}$, $\Phi_{s\beta}$ and calculated sizes of the current, $I_{s\alpha}$, $I_{s\beta}$)

$$T_e = \frac{3}{2} p [\Phi_{s\alpha} i_{s\beta} - \Phi_{s\beta} i_{s\alpha}] \quad (13)$$

The switching table allows to select the appropriate inverter switching state according to the state of flux hysteresis comparator (Cflx) and torque hysteresis comparator (Ccpl) and the sector (N) where is the stator vector flux (Φ_s) in the plan (β , α), in order to maintain the magnitude of stator flux and electromagnetic torque inside the hysteresis bands. The above consideration allows construction of the switching table as presented in Table 1 [2].

TABLE 1. SWITCHING TABLE FOR CLASSICAL DTC

N		1	2	3	4	5	6
Cflx	Ccpl						
1	1	2	3	4	5	6	1
	0	7	0	7	0	7	0
	-1	6	1	2	3	4	5
0	1	3	4	5	6	1	2
	0	0	7	0	7	0	7
	-1	5	6	1	2	3	4

The voltage vector table receives the flux level, the torque level and the sector number and generates appropriate control for the inverter from a look-up table as in Table 1[3].

Table 1 can be simply modified by applying zero voltage vectors (V_0 , V_7) for the torque decrease states (-1), and this modification will result in decreasing the torque ripple largely, a considerable reason for this decrease is that applying the zero voltage vectors result in reducing the inertia of the motor at this instant and this result in reducing the torque with a percent which is more suitable than the percent given by applying the vectors in Table 1 for the torque decrease states [3]. Table 2 illustrates this modification.

TABLE 2. SWITCHING TABLE FOR NEW SWITCHING TABLE OF CLASSICAL DTC

N		1	2	3	4	5	6
Cflx	Ccpl						
1	1	2	3	4	5	6	1
	0	1	2	3	4	5	6
	-1	7	0	7	0	7	0
0	1	3	4	5	6	1	2
	0	0	7	0	7	0	7
	-1	0	7	0	7	0	7

V. DTC USING NEURAL NETWORK

In order to improve the two-level DTC performances a complimentary use of neural networks controller is proposed. ANN is part of the family of statistical learning methods inspired by biological nervous system and are used to estimate and approximate functions that depends only on a large number of inputs [6].

A group of artificial neurons, which work in parallel, their inputs and outputs have the same destination from a layer.

Each neural network must contain at least one layer of neurons but can join as many as someone projects. The layer gathering the neurons which give the output of the neural networks is called output layer. Layers which contain the neurons interposed between the global inputs of the neural network and the inputs of the neurons from the output layer are called hidden layers. Usually, there are used feed-forward NN which contains a hidden layer and an output layer [7].

The Principle of neural order DTC (DTC-ANN) consists with replaced the table of commutation by the neural controller. As shown in Fig. 4.

Table 3 summarizes all of the parameters of the LM for control classical DTC and new switching table of classical DTC.

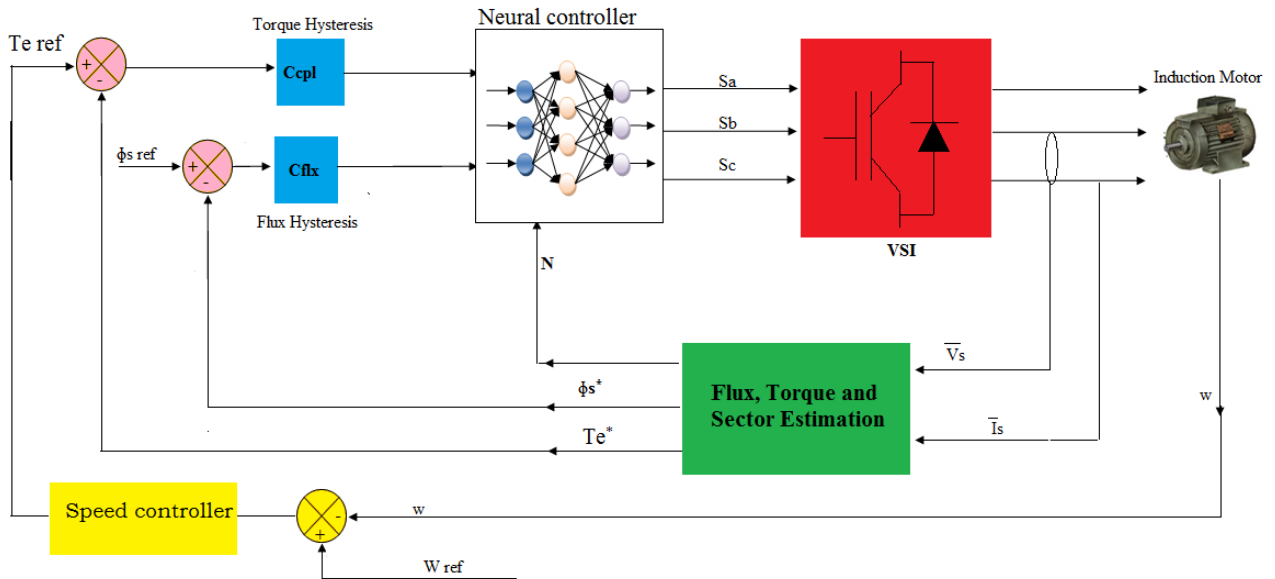


Fig. 5. DTC with ANN

TABLE 3. PARAMETERS OF THE LM FOR NEW SWITCHING TABLE AND CLASSICAL DTC

Parameters of the LM	values
Number of hidden layers	30
Pas d' training	0.002
Pas d' posting (posting of the error per pieces)	50
Iteration count (epochs)	2000
Coeff of acceleration of convergence (mc)	0.9
Error (goalkeeper)	0
Functions of activation	Tansig, Purelin

The convergence of the network in summer obtained by using the values of the parameters grouped in the Table 3.

In Matlab command we generated the Simulink block ANN of switching table by 'gensim' given this model show Fig.6

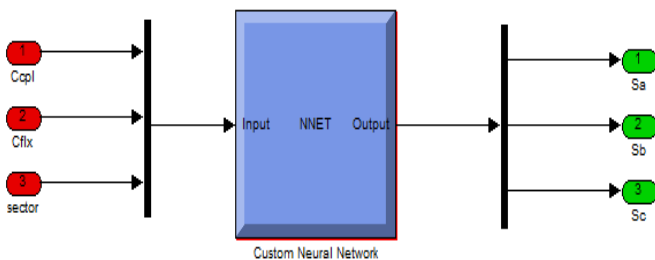


Fig. 6. Simulink block for ANN switching table

The block neural network content two layer 1 and layer 2 shows Fig.7.

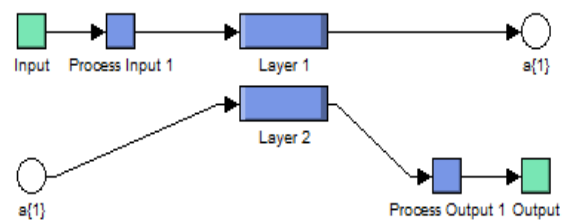


Fig. 7. Block neural network.

VI. DTC CONTROL WITH NEURAL HYSTERESIS COMPARATORS

For order DTC with neural hysteresis comparators, one will keep same work that with the classical DTC but we change that the hysteresis comparators (comparators of the torque and flux) by two regulators containing networks of neurones as is illustrated in Fig. 8.

Table 4 and Table 5 summarize all of the parameters of the LM for neural hysteresis comparators of the torque and flux.

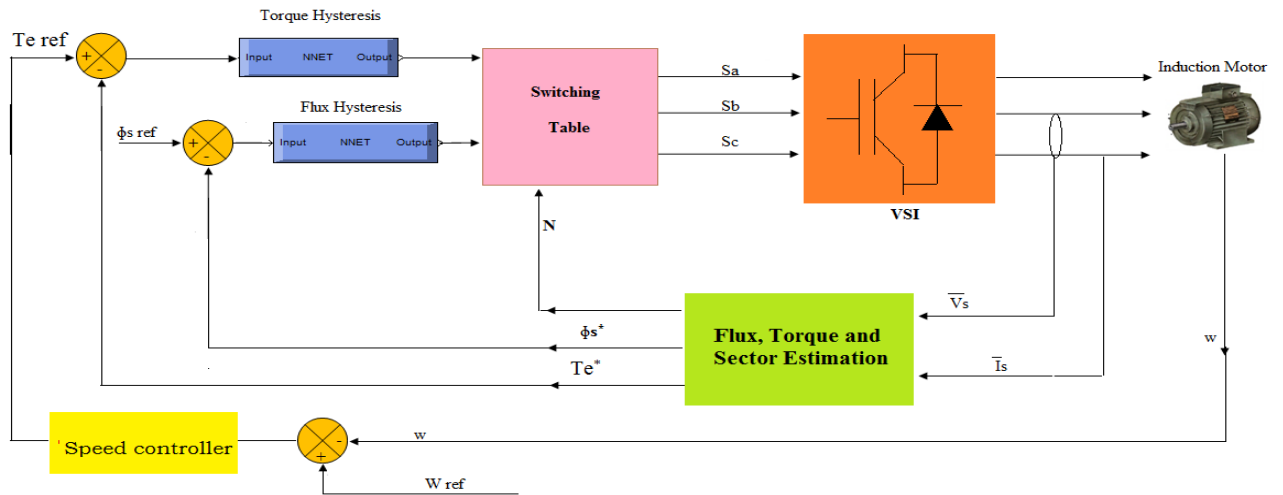


Fig. 8. DTC with neural hysteresis comparators

TABLE 4. PARAMETERS OF THE LM FOR TORQUE HYSTERESIS COMPARATOR

Parameters of the LM	values
Number of hidden layer	4
Pas d' training	0.002
Pas d' posting (posting of the error per pieces)	50
Iteration count (epochs)	5000
Coeff of acceleration of convergence (mc)	0.9
Error (goalkeeper)	0
Functions of activation	Tensing, Purling

TABLE 5. PARAMETERS OF THE LM FOR FLUX HYSTERESIS COMPARATOR

Parameters of the LM	values
Number of hidden layer	3
Pas d' training	0.002
Pas d' posting (posting of the error per pieces)	50
Iteration count (epochs)	5000
Coeff of acceleration of convergence (mc)	0.9
Error (goalkeeper)	0
Functions of activation	Tensing, Purling

VII. DTC CONTROL WITH FUZZY SPEED CONTROLLER

All the schemes cited above use a PI controller for speed control. The use of PI controller to command a high performance direct torque controlled induction motor drive is often characterised by an overshoot during start up. This is mainly caused by the fact that the high value of the PI gains needed for rapid load disturbance rejection generates a positive high torque error. This will let the DTC scheme take control of the motor speed driving it to a value corresponding to the reference stator flux [8].

At start up, the PI controller acts only on the error torque value by driving it to the zero border. When this border is crossed, the PI controller takes control of the motor speed and drives it to the reference value.

In this paper, a variable gain fuzzy PI controller is used to replace the classical PI controller in the speed control of a new strategy of classical DTC controlled induction machine. The fuzzy control is basically nonlinear and adaptive in nature, giving robust performance under parameter variation and load disturbance effect [9].

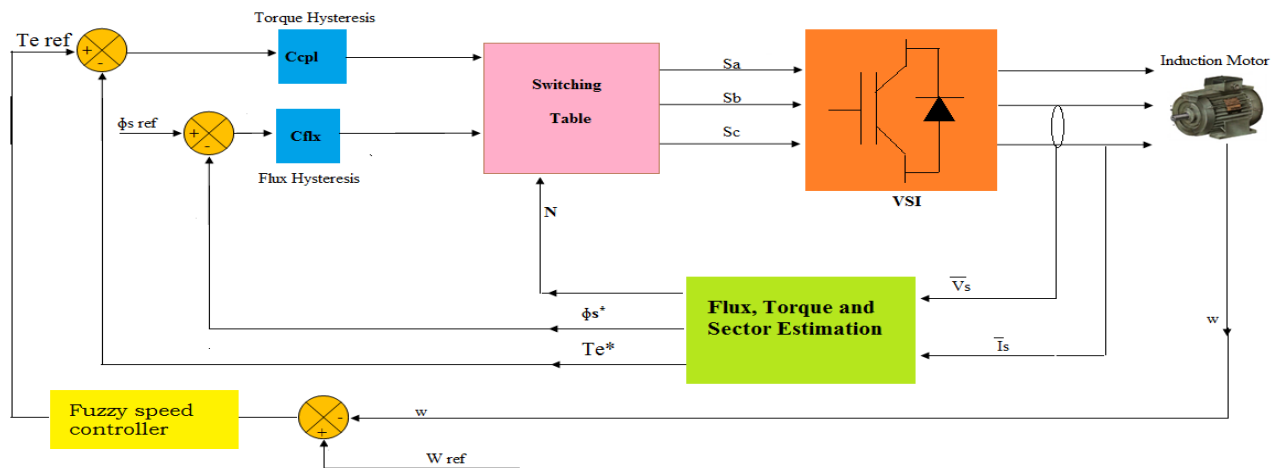


Fig. 9. DTC with fuzzy PI controller

The fuzzy controller design is based on intuition and simulation. These values compose a training set which is used to obtain the table of rules [10]. The block diagram of the Fuzzy PI controller is shown in Fig. 10.

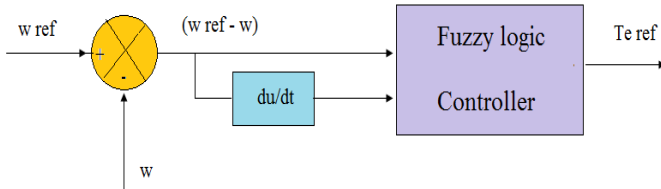


Fig. 10. Fuzzy logic control of speed.

One possible initial rule base, that can be used in drive systems for a fuzzy logic controller, consist of 49 linguistic rules, as shown in Table 2 [11, 12], and gives the change of the output of fuzzy logic controller in terms of two inputs: the error ($e = W_{ref} - W$) and change of error (Δe). Fig. 11 and 12 shows the membership functions of input and output variables respectively.

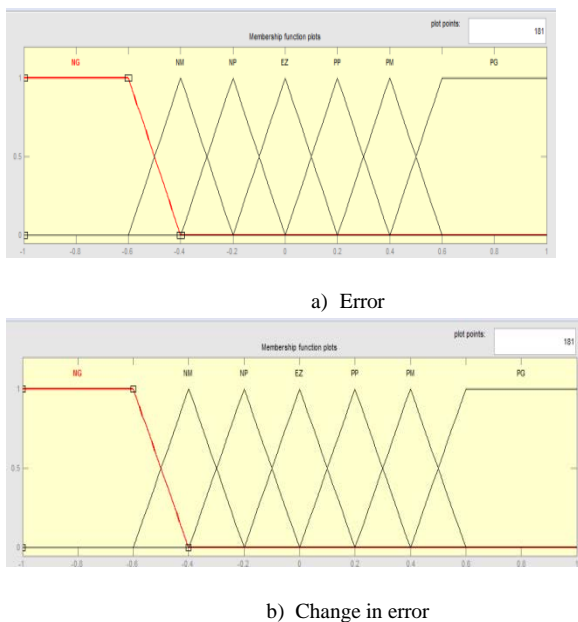


Fig. 11. Input variables membership functions.

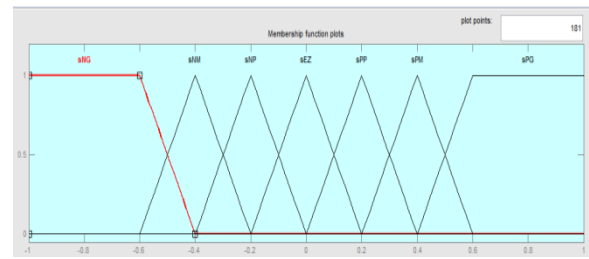


Fig. 12. Fuzzy function for output.

TABLE 6. RULE BASE FOR THE FUZZY CONTROLLER

e	NL	NM	NP	EZ	PS	PM	PL
Δe	NL	NM	NP	EZ	PS	PM	PL
NL	NL	NL	NL	NL	NM	NP	EZ
NM	NL	NL	NL	NM	NP	EZ	PS
NP	NL	NL	NM	NP	EZ	PS	PM
EZ	NL	NM	NP	EZ	PS	PM	PL
PS	NM	NP	EZ	PS	PM	PL	PL
PM	NP	EZ	PS	PM	PL	PL	PL
PL	EZ	PS	PM	PL	PL	PL	PL

VIII. DTC CONTROL BASED ON NEURAL HYSTERESIS COMPARATORS AND FUZZY SPEED CONTROLLER

The principle of fuzzy logic and neural networks (neural hysteresis comparators) direct torque control similar to traditional DTC. The difference is using a fuzzy logical controller and neural networks controllers to replace the classical PI controller, and hysteresis comparators respectively. As shown in Fig.13.

IX. MACHINE PARAMETERS

The motor parameters are Power = 1MW, Rated voltage = 791V, Poles = 3, Frequency=60Hz, Stator resistance = 0.228ohm, Rotor resistance = 0.332ohm, Stator inductance = 0.0084H, Rotor inductance = 0.0082H, Inertia = 20 Kg.m², Mutual inductance = 0.0078H.

X. SIMULATION RESULTS

Reference speed is chosen as 1000 r.p.m, while external load torque is balanced between 0, 6500 N.m and -6500 N.m applied at 0.8s, 1.8s respectively.

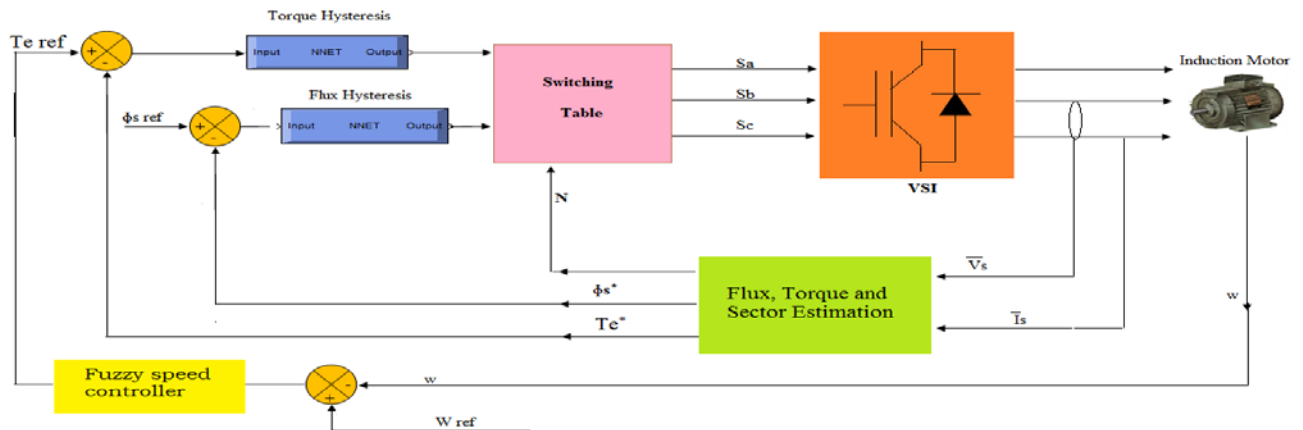


Fig. 13. DTC with neural hysteresis comparators and fuzzy speed controller.

To test the performances of the used control schemes, the simulation of the system was realised using the matlab tool. Figures 14-20 show simulations of the classical DTC, the new switching table of DTC, DTC-ANN, the new switching table of DTC with ANN, the new switching table of DTC with neural hysteresis comparators, the new switching table of DTC with fuzzy speed controller and the new switching table of DTC with neural hysteresis and fuzzy speed controller.

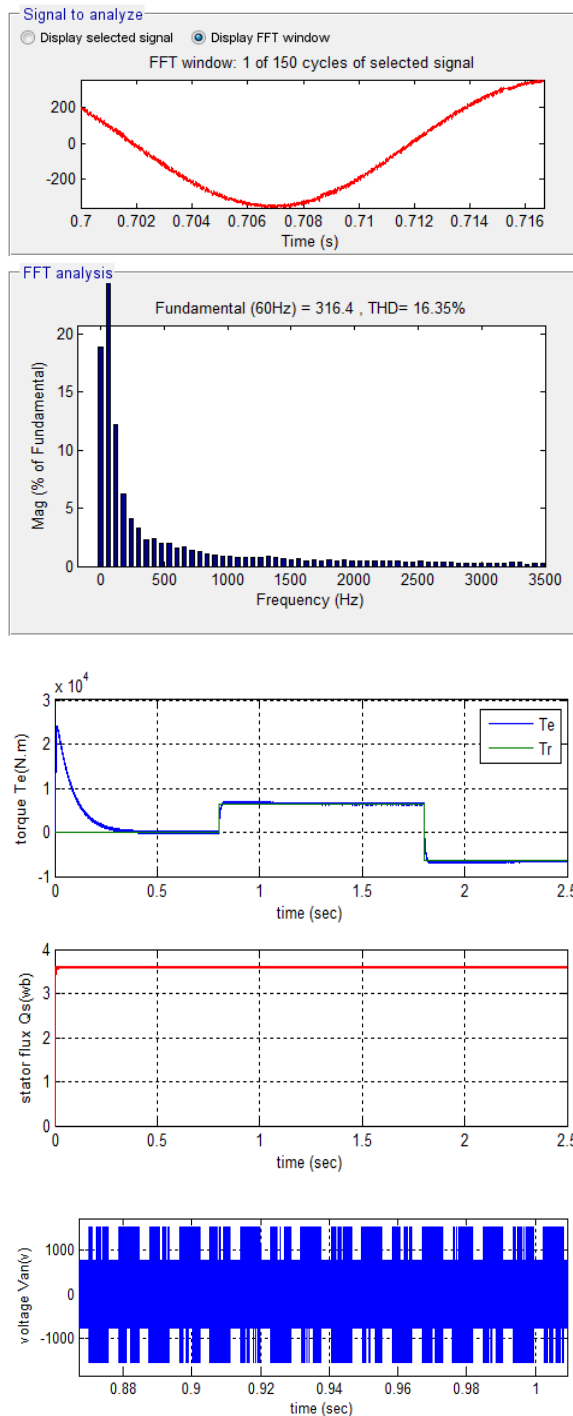


Fig. 14. Dynamic responses of Classical DTC

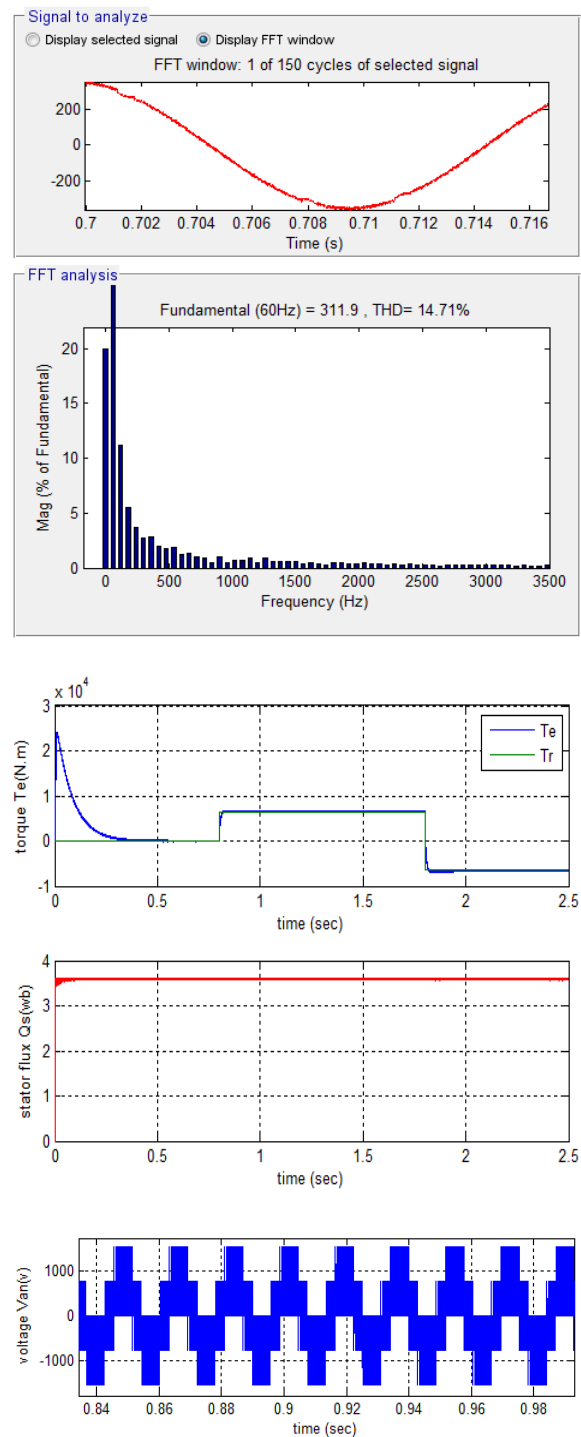


Fig. 15. Dynamic responses of new switching table of classical DTC

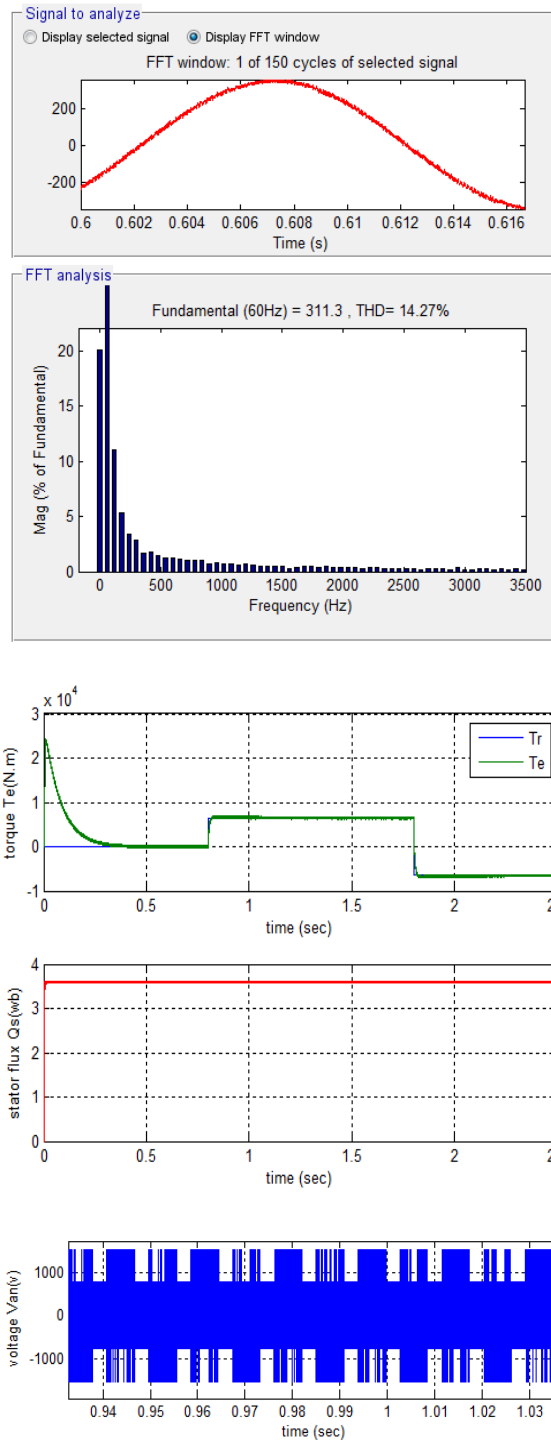


Fig. 16. Dynamic responses of Classical DTC-ANN

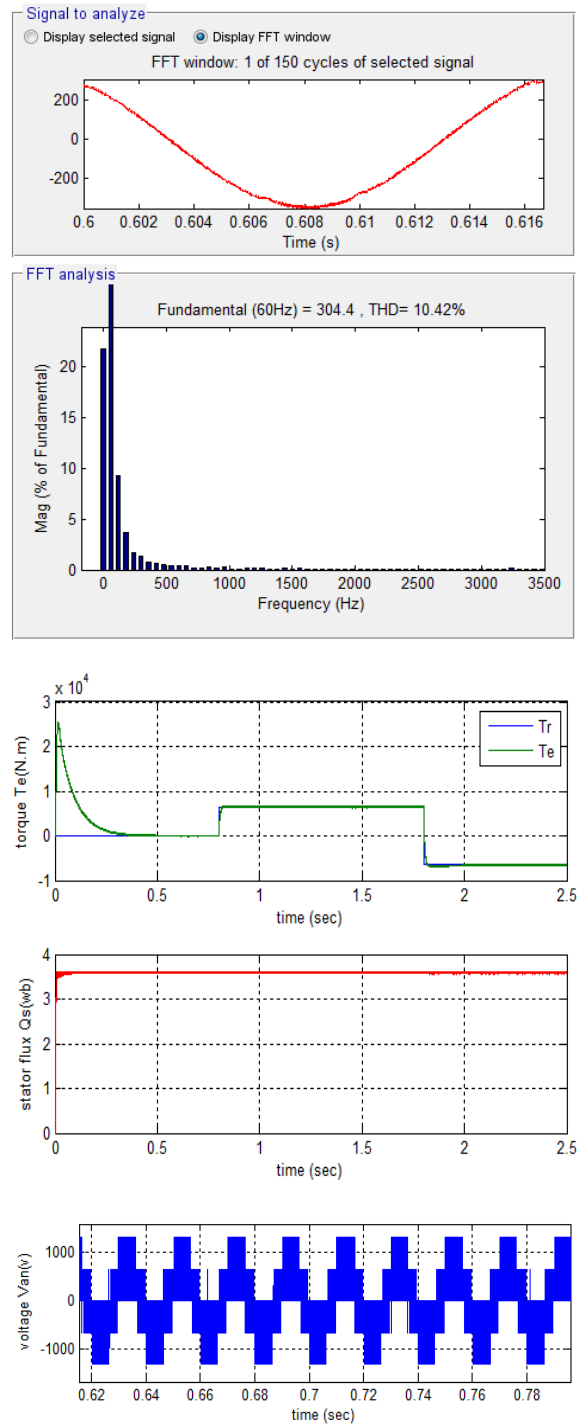


Fig. 17. Dynamic responses of new switching table with ANN

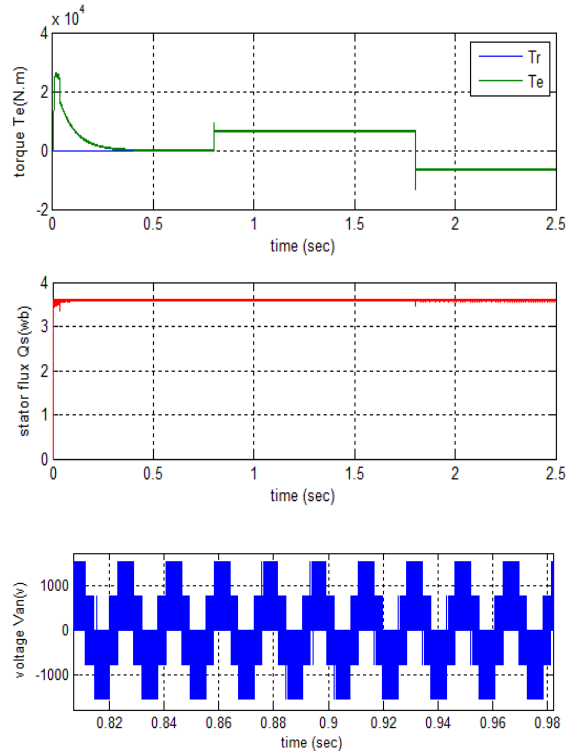
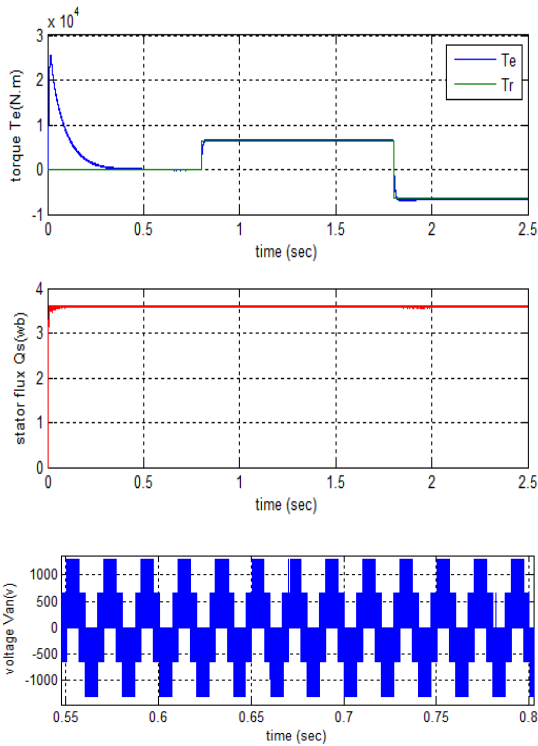
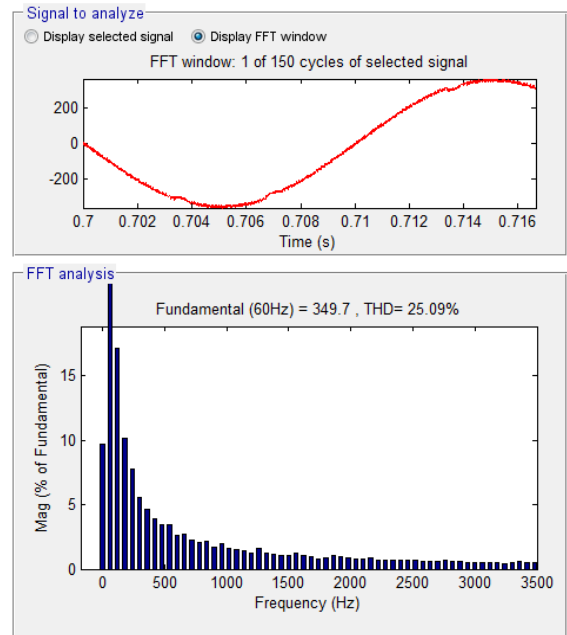
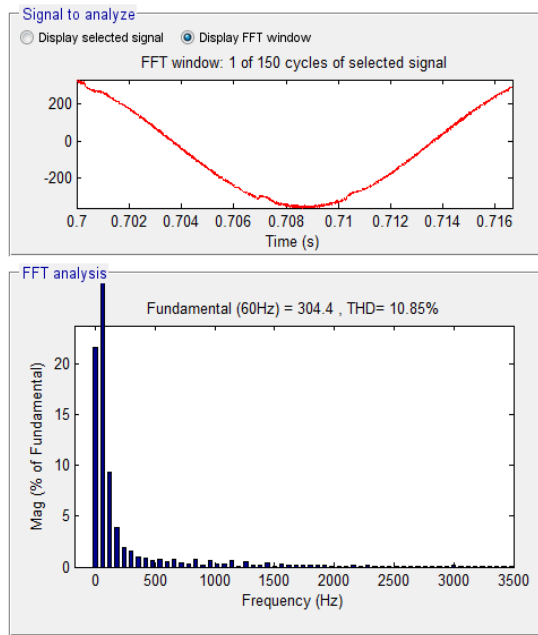
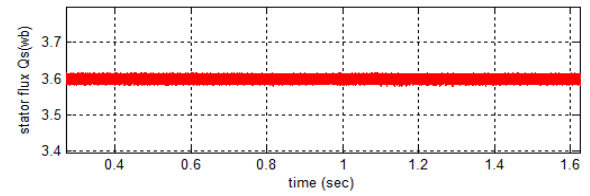
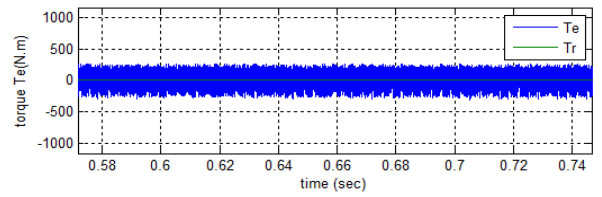
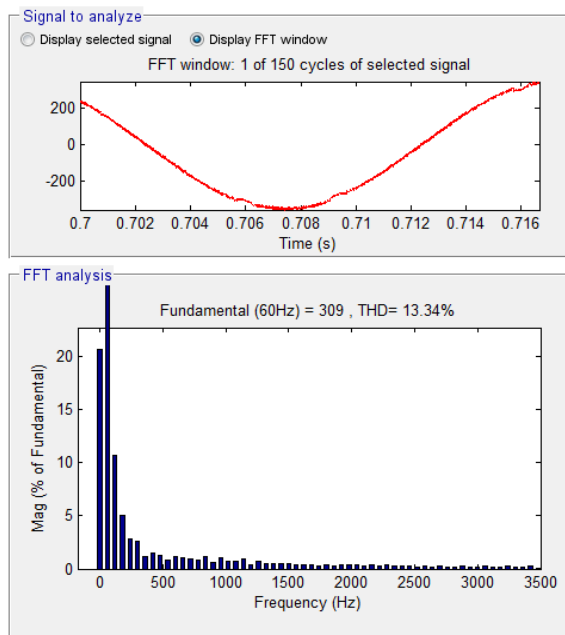
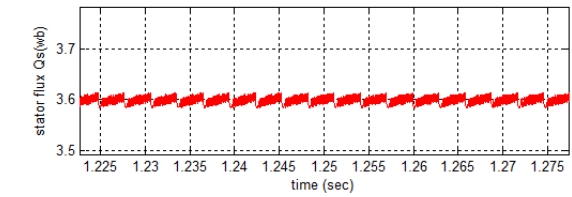
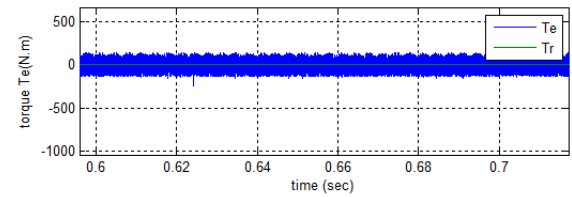


Fig. 18. Dynamic responses of new switching table with neural hysteresis comparators

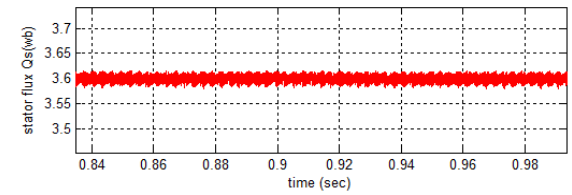
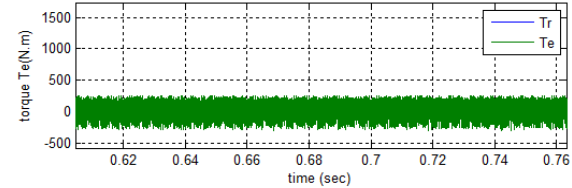
Fig. 19. Dynamic responses of new switching table with fuzzy speed controller



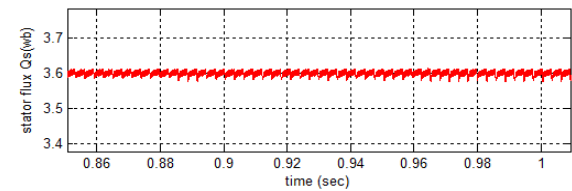
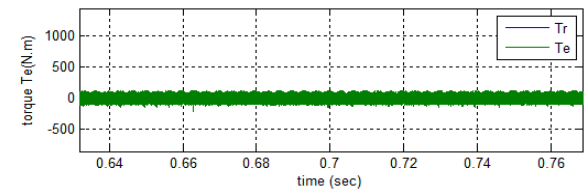
a) Classical DTC



b) New switching table of DTC



c) Classical DTC with ANN



d) New switching table with ANN

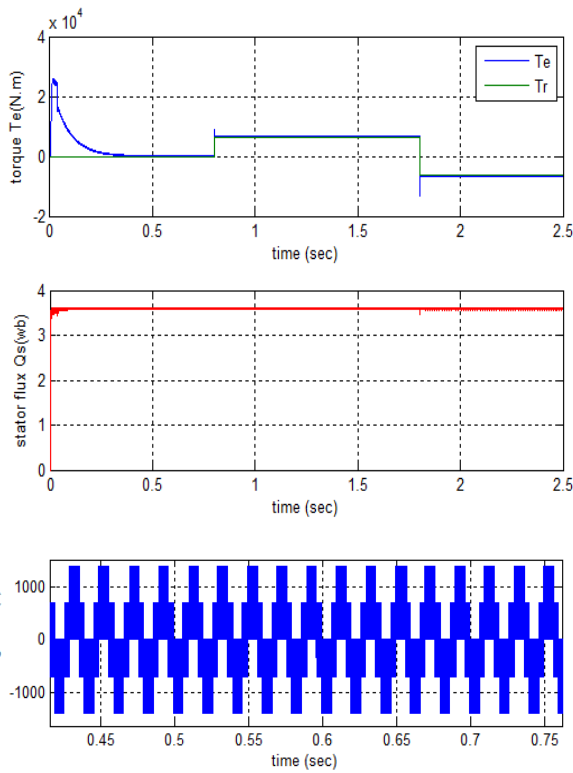
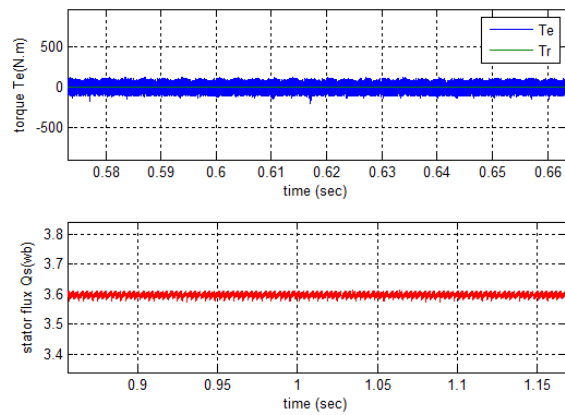
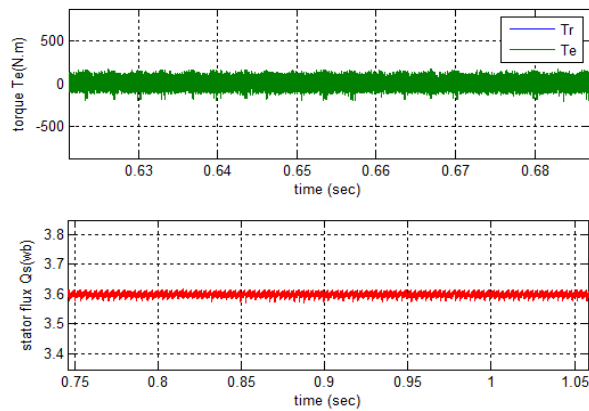


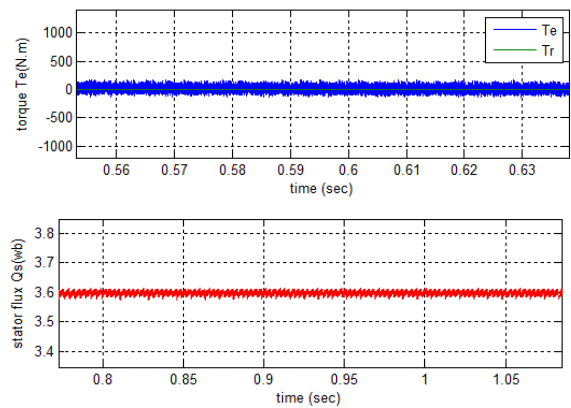
Fig. 20 Dynamic responses of new switching table with neural hysteresis comparators and fuzzy speed controller.



e) New switching table based on neural hysteresis comparators



f) New switching table based on fuzzy speed controller



g) New switching table of DTC with neural hysteresis comparators and fuzzy speed controller

Fig. 21. Comparison between the proposed strategies.

To compare with classical DTC and the new strategy of DTC proposed for IM drives using artificial neural networks, fuzzy speed controller, and neural hysteresis comparators are simulated. The dynamic responses of speed, flux, torque and stator current for the starting process with $[0 \rightarrow 6500 \rightarrow 6500]$ N.m load torque applied and a constant command flux of 3.6Wb are shown in figure from 14 to 20 respectively.

TABLE 7. COMPARAISON RESULTS

Control	Ias THD (%)
Classical DTC	16.35
New strategy of DTC	14.71
Classical DTC with ANN	14.27
New strategy of DTC with ANN	10.42
New strategy of DTC with neural hysteresis comparators	10.85
New strategy of DTC with fuzzy speed controller	25.09
New strategy of DTC with neural hysteresis comparators and fuzzy speed controller	13.34

The torque waveform of classical DTC scheme contains large amount of high frequency ripples and it is also reflected in the current waveform. It is clear from the simulation results of the new strategy of DTC scheme, the torque and current ripples have been reduced. While simulating the classical DTC of IM, the ripple content obtained was about 40% and by the proposed new strategy of DTC scheme, the ripple content has been successfully reduced to about 10%.

The simulation results in Fig. 21 (a, b) show the response of electromagnetic torque and stator flux of the classical DTC, and the new strategy of DTC respectively. It can be seen that the torque ripples, flux ripples with the new strategy of DTC in steady state are significantly reduced compared to classical DTC.

The simulation results in Fig. 21 (b, d) show the response of electromagnetic torque and stator flux of the new strategy of DTC, and new strategy of DTC with ANN respectively. It can be seen that the torque ripples, flux ripples with the new strategy of classical direct torque control with ANN in steady state are significantly reduced compared to the new strategy of DTC.

The simulation results in Fig. 21 (a, b, c, e, f) show the response of electromagnetic torque and stator flux of the classical DTC, and new strategy of DTC, and new strategy of classical DTC with neural hysteresis comparators, and the new strategy of DTC with neural hysteresis comparators, and the new strategy of DTC with fuzzy speed controller respectively. It can be seen that the torque ripples and flux ripples with the new strategy of DTC with neural hysteresis comparators in steady state are significantly reduced compared to others controls.

The simulation results in Fig. 21 (a, b, c, f, g) show the response of electromagnetic torque and stator flux of the classical DTC, and new strategy of DTC, and classical DTC with ANN, and new strategy of DTC with fuzzy speed controller, and new strategy of DTC with neural hysteresis comparators and fuzzy speed respectively. It can be seen that the torque ripples and flux ripples with the new strategy of DTC with neural hysteresis comparators and fuzzy speed controller in steady state are significantly reduced compared to others controls.

XI. CONCLUSIONS

The DTC represents a viable alternative to field oriented control being also a general philosophy for the AC drives. The DTC was introduced to give a fast and good dynamic torque

of an IM, it does not require any mechanical sensor in the rotor comparatively to the conventional methods. Its high dynamic response is due to the absence of the current regulator normally used in torque controllers.

In this paper, the new switching table of DTC is presented and it is shown that with intelligent techniques (Neural network, fuzzy logique) for IM drives fed by two-level inverter. The simulation results obtained for the new switching table of DTC with ANN illustrate a considerable reduction in stator flux ripple, THD value of stator current and torque ripple compared to the existing classical DTC, DTC with ANN, DTC with neural hysteresis comparators, DTC with fuzzy speed controller, neural hysteresis DTC with fuzzy speed controller utilizing two-level inverter.

REFERENCES

1. A. Chikhi, "Direct torque control of induction motor based on space vector modulation using a fuzzy logic speed controller," *Jordan Journal of Mechanical and Industrial Engineering*, Vol. 8, No. 3, pp: 169-176, 2014.
2. R. Sadouni, A. Meroufel, "Performances comparative study of field oriented control (FOC) and direct torque control (DTC) of dual three phase induction motor (DTPIM)," *International Journal of Circuits, Systems and Signal Processing*, Vol. 6, Issue 2, 2012.
3. A. Hassan Adel, S. Abo-zaid, A. Refky, "Improvement of direct torque control of induction motor drives using Neuro-Fuzzy controller," *Journal of Multidisciplinary Engineering Science and Technology (JMEST)*, Vol. 2, Issu 10, October 2015.
4. J. L. Azcue, A. J. Segurezi Filho, E. Ruppert, "Self-Tuning PI-type fuzzy direct torque control for three-phase induction motor," *Wseas Transactions on Circuits and Systèmes*, Issue 10, Vol. 11, October 2012.
5. R. Toufouti S. Meziane, H. Benalla, "Direct torque control for induction motor using intelligent techniques," *Journal of Theoretical and Applied Information Technology (JATIT)*, 2007.
6. D. Narasimha Rao, T. Surendra, S. Tara Kalyani, "DPFC performance with the comparison of PI and ANN controller," *International Journal of Electrical and Computer Engineering (IJECE)*, Vol. 6, No. 5, pp: 2080-2087, October 2016.
7. D. D. Micu, L. Czumbil, G. Christoforidis, E. Simion, "Neural networks applied in electromagnetic interference problems," *Rev. Roum. Sci. Techn.-Electrotechn. Et Energ.*, Vol. 57, No. 2, pp: 162-171, 2012.
8. A. Miloudi, E. A. Al-Radadi, A. Draou, "A variable gain PI controller used for speed control of a direct torque neuro fuzzy controlled induction machine drive," *Turk. J. Elec. Engin.*, Vol. 15, No. 1, 2007.
9. A. Tahour, H. Abid, A. G. Aissaoui, M. Abid, « Fuzzy controller of switched reluctance motor, » *Acta Electrotehnica*, Vol. 47, No. 3, pp : 124-131, 2006.
10. L. Youb, A. Craciunescu, « Direct torque control of induction motors with fuzzy minimization torque ripple, » *Proceedings of the World Congress on Engineering and Computer Science*, Vol. 2, 2009.
11. H. Benbouhenni, "Comparateur à hysteresis à sept niveaux pour la commande DTC basée sur les techniques de l'intelligence artificielle de la MAS," *Journal of Advanced Research in Science and Technology*, Vol. 4, No. 2, pp: 553-569, 2017.
12. M. Abdelhafidh, "Stratégies de commande DTC-SVM et DPC appliquées à une MADA utilisée pour la production d'énergie éolienne," *Thèse de Doctorat, Ecole Nationale Polytechnique, Alger*, 2014.